Vehicle and Occupant Motion in Far-Side Impacts

Sean H. Haight and Kennerly H. Digges
National Crash Analysis Center
George Washington University
Washington, DC
December 2010

ABSTRACT

Side impact crash tests are commonly performed in research as well as a part of the New Car Assessment Program (NCAP). For example, in the NCAP 214 side impact test the test protocol indicates that two near-side occupants are to be used in such testing. Therefore, far-side occupant research is rarely conducted. Two crash tests were conducted to determine the occupant kinematics of a far-side occupant. In addition, the effects of impact positions, rotation, and seatbelt performance were analyzed with regard to the far-side occupant.

Analyses of the rotation of the vehicles showed that the impact point affects the magnitude and direction of yaw during the collision. The vehicle motion affects the occupant motion relative to the vehicle. When the impact was centered on the B-pillar, the occupant moved toward the A-pillar. When the impact was centered on the A-pillar, the occupant motion was in a more lateral direction.

BACKGROUND

A far-side impact can be described as a collision in which an occupant is seated on the side of the vehicle that is opposite the impact location. For example, one far side scenario could be an occupant sitting in the driver seat, while being struck on the passenger side of the vehicle.

This research is a continuation of an earlier project to develop the technology base for far-side protection. The project was managed jointly by Monash University in Australia and George Washington University in the US. [Fildes and Digges 2009]. This earlier project determined the crash environment associated with serious injuries in far-side crashes and developed a technical basis for the crash dummies, injury criteria, and test procedures to be used in evaluating far-side countermeasures. The results of the project and the published literature it produced are contained in an ESV paper by Digges [2009].

An in-depth analysis of the crash environment for belted occupants in far-side crashes was presented in earlier papers [Digges, 2006, Gabler, SAE 2005 and ESV 2005]. The analysis indicated that for belted occupants with MAIS 3+ injuries, the 50% median crash severity was a lateral delta-V of 28 km/h and an extent of damage of 3.6 as measured by the CDC scale [SAE Standard J224, Collision Deformation Classification]. The most frequent damage area for seriously injured belted occupants was the front 2/3 of the vehicle (42%), followed by the rear 2/3 (21%). The most frequent principal direction of force (PDOF) was 60° (60%), followed by 90° (24%). The head and chest were the most frequently injured body regions, each at about 40% [Gabler 2008]. The injuring contacts that most frequently caused chest injury were the struck-side interior (23.6%), the belt or buckle (21.4%) and the seat back (20.9%) [Fildes, 2007]. A Harm analysis showed 30% of the Harm associated with side impact crashes occurred to the far side occupant and that this figure was reasonably consistent in both the US and Australia [Gabler, Firzharris, et al 2005].

Sled tests that compared the kimnematics of dummies and cadavers were conducted by the Medical College of Wisconsin [Pintar 2006, 2007]. A conclusion of this research was: "The THOR and WorldSID dummies demonstrate adequate biofidelity to develop countermeasures in this (far-side) crash mode" [Pintar 2007].

The sled tests conducted by Pintar did not include any rotation of the sled during the impact. However, MADYMO computer simulations by Cuadrado found that vehicle rotation could influence the occupant kinematics in far-side crashes [Cuadrado 2008, 2010]. The simulations by Cuadradro were limited by the small number of crash tests that have been conducted under the most frequent far-side crash modes. Data from the crash tests are needed to provide the vehicle translation and rotation to the MADYMO model.

A limited number of crash tests to support the understanding of far-side occupant kinematics have recently been reported [Smyth 2007 and Newland 2008]. The NCAC tests reported in this paper are a continuation of the research in far-side testing.

Currently, the Federal Motor Vehicle Safety Standards (FMVSS) require specific side impact protection for occupants in near-side impacts. However, there is no regulation for far-side impacts. Opportunities for safety improvements exist because far-side occupants account for up 30% of injuries in real world side impact collisions [Fildes 2000]. In Australia, where belt use is over 90%, head injuries occurred in higher frequencies in far-side collisions when compared to near-side collisions [Fildes 1994].

Since FMVSS 214 side impact occupant protection requirements only test the near side occupant there are limited studies and tests in this crash scenario and more research should be performed to analyze how the occupant moves when being struck from the far-side. This study continues the research in this crash scenario. The National Crash Analysis Center performed two far-side crash tests to analyze the kinematics of occupants seated in this configuration. Based on earlier research an angular crash is most frequently involved in MAIS 3+ injuries for belted occupants exposed occupants in far-side crashes. However, the location of the impact along the side of the vehicle can produce different vehicle intrusion patterns and different linear and angular vehicle kinematics. The goals of the tests were to understand how two different impact locations affect the motion of the vehicle and the occupant relative to the vehicle. Some important factors to be studied include the vehicle rotation, the head impact location and the seatbelt performance. These two tests were further analyzed to meet the goals of the study.

CRASH TESTS

Two crash tests were performed in 2010 at the FHWA – Federal Outdoor Impact Laboratory in McLean, VA. The first test was numbered #10010 and the second test was numbered #10016. These numbers will be used throughout the study to refer to the specific test being analyzed.

Test 10010 – B- pillar impact point

The first test was designed to be a passenger side impact at a speed of 62 kph (38.5 mph). The bullet vehicle for this crash test was a 1996 Ford Explorer (four door) and the target vehicle was a 1997 Ford Taurus. The occupant in the Taurus was a Hybrid II, non-instrumented anthropomorphic test device (ADT). The occupant was placed on the driver side of the Taurus. Additionally, the Taurus was positioned at 60 degrees to the test track and the impact point was set so that the first point of contact with the Explorer would be at the Taurus B-pillar.

Instrumentation for test 10010 consisted of two sets of tri-axial accelerometers at the center of gravity as well as a set of rotation sensors that measured roll, pitch and yaw. Seven high speed video recorders were placed around the target vehicle as well as one placed on the hood of the Taurus to capture the motion of the occupant. Two real time videos were used as well.
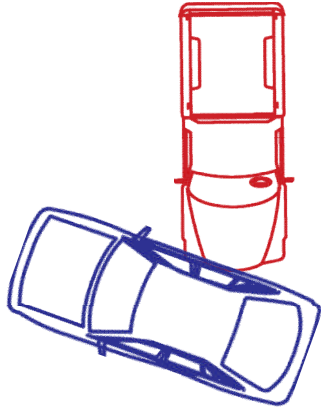
Figure 1: Test configuration for Test 10010, B- pillar impact point; 60 degree; Hybrid II ADT occupant (un-instrumented)

Test 10016 – A- pillar impact point

The second test was also designed to be a passenger side impact at a speed of 62 kph (38.5 mph). The bullet vehicle for this test was the same vehicle used in test 10010. However, the damaged components were replaced with new, undamaged parts. The target vehicle for test 10016 was a 2002 Ford Taurus. The occupant in the Taurus was a Hybrid III, instrumented, anthropomorphic test device (ADT). The occupant was placed in the driver side of the Taurus and the vehicle was angled at 60 degrees. Explorer was aligned so that the center would impact the A- pillar of the Taurus.

Instrumentation for test 10016 consisted of two sets of tri-axial accelerometers at the center of gravity as well as two sets of rotation sensors that measured roll, pitch and yaw. In addition, 40 data channels recorded data from the ADT including head and pelvis accelerations. Seven high speed video recorders were placed around the target vehicle as well as one placed on the hood of the Taurus to capture the motion of the occupant.
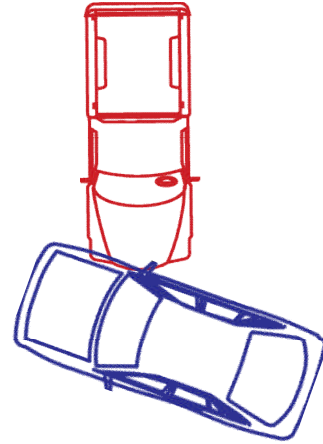
Figure 2: Test configuration for Test 10016, A- pillar impact point; 60 degree; Hybrid III ADT occupant

TEST RESULTS

Test 10010 - B- pillar impact point

Figure 3 shows the recorded accelerometer data and the calculated change in velocity for the Ford Taurus.
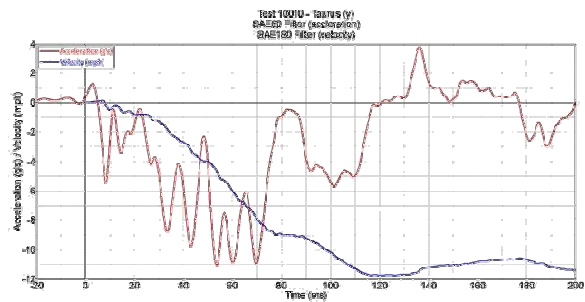
Figure 3: Acceleration and velocity data for the Ford Taurus (Test 10010)

The recorded data, filtered with a class SAE60 filter [SAE J211, 1988] shows a max acceleration of 11 g's at 52 ms. The maximum change in velocity (delta-v) was calculated to be 18.9 kph (11.8 mph). The crash pulse duration was about 115 ms.

Test 10016 – A- pillar impact point

Figure 4 shows the recorded accelerometer data and the calculated change in velocity for the Ford Taurus
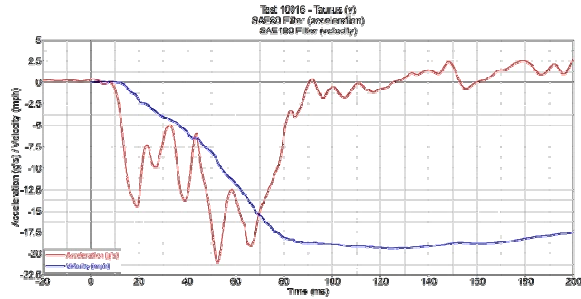
Figure 4: Acceleration and velocity data for the Ford Taurus (Test 10016)

The recorded data, filtered with a class SAE60 filter, shows a max acceleration of 21 g's at 52ms. The delta-v was calculated to be 29.7 kph (18.5 mph). The crash pulse duration was about 80 ms.

Figure 5 shows the recorded Hybrid III ADT head resultant data filtered with a class SAE1000 filter. The maximum resultant head acceleration for the occupant is 20 g's at 145 ms. The calculated Head Injury Criteria (32 ms) is 58.8.
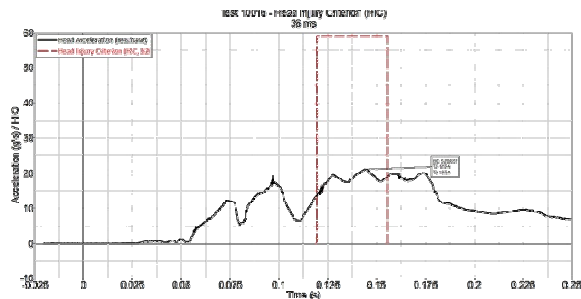
Figure 5: Resultant head acceleration for the Hybrid III ADT occupant (Test 10016)
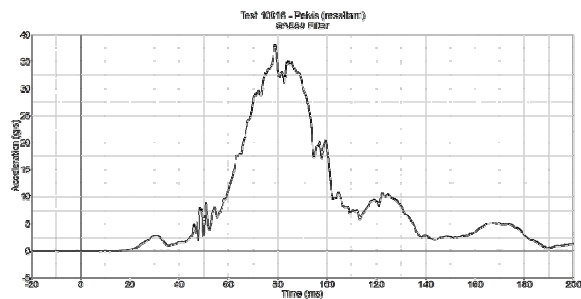
Figure 6: Resultant pelvis acceleration for the Hybrid III ADT occupant (Test 10016)

Figure 6 shows the recorded Hybrid III ADT pelvis resultant data also filtered with a class SAE1000 filter. The maximum resultant acceleration for the pelvis was recorded as 38 g's at 78 ms.

MADYMO MODELING

The use of Mathematical Dynamic Modeling (MADYMO) is frequently used as a tool to simulate impacts and occupant kinematics. For this study, a MADYMO system model was created using the interior of a Ford Taurus and a human model. Figure 7 shows the model configuration for the two tests in the study.

Figure 7: The configuration of the MADYMO model for simulation of the two tests in the study

For these tests, the data from the tri-axial accelerometers were used in conjunction with the data from the yaw rate sensor as inputs for the MADYMO model.

Overhead pictures from the 10010 B-pillar crash are shown at contact (Figure 8) and at 200 ms (Figure 9). The location of the occupant in the MADYMO model after 200 ms for test 10010 can be seen in Figure 10. Overhead pictures from the 10016 A-pillar crash are shown at contact (Figure 11) and at 200 ms (Figure 12) The location of the occupant in the MADYMO model after 200 ms for test 10010 can be seen in Figure 13.

Figure 8: Overhead view of test at impact (Test 10010) B-pillar impact

Figure 11: Overhead view of test at impact (Test 10016) A-pillar impact

Figure 9: Overhead view of test 200 ms after impact (Test 10010) B-pillar impact
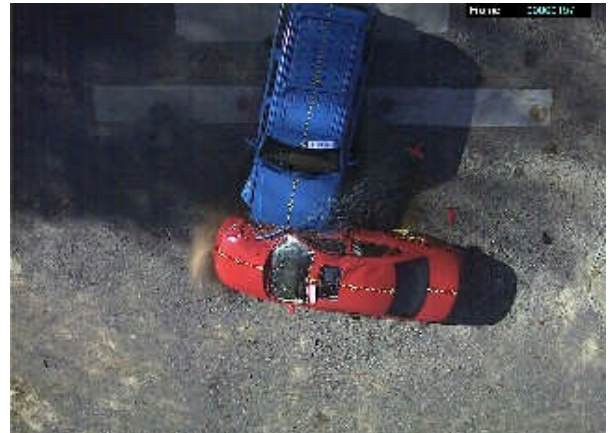
Figure 12: Overhead view of test 200 ms after impact (Test 10010) A-pillar impact
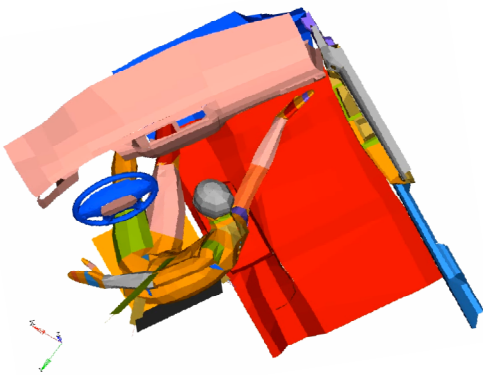
Figure 10: Graphic results from MADYMO model 200 ms after impact (Test 10010) B-pillar impact
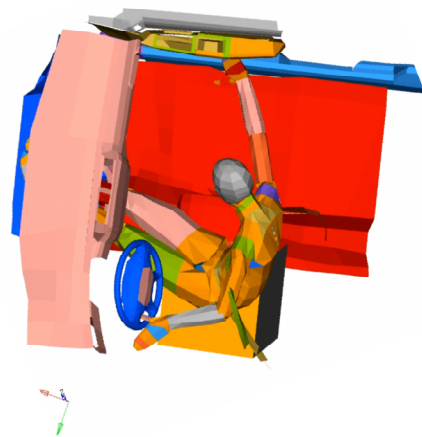
Figure 13: Graphic results from MADYMO model 200 ms after impact (Test 10010)

Figures 14 and 15 show frontal views of the MADYMO simulations of the two tests.
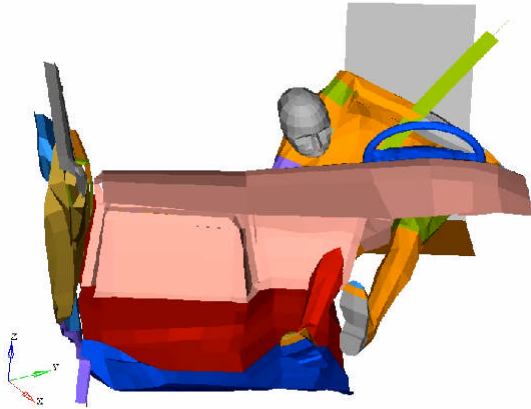
Figure 14: Graphic results from MADYMO model 200 ms after impact (Test 10010) B-pillar impact

T
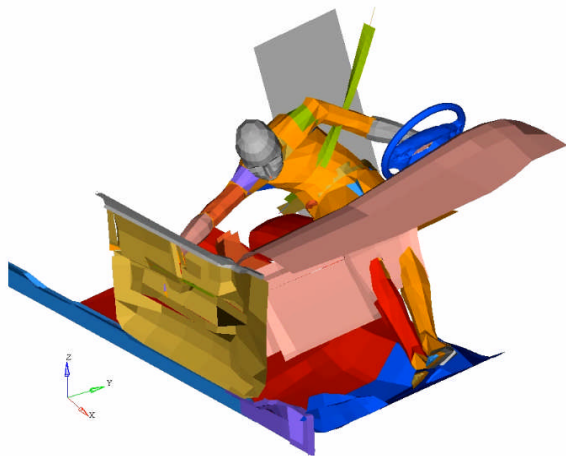
Figure 15: Graphic results from MADYMO model 200 ms after impact (Test 10016) A-pillar impact

DISCUSSION

Rotation analysis

Since both crash tests had different impact points relative to the center of gravity, the rotation about the vertical axis differs. For test 10010, the B- pillar impact point, the rotation was positive. Since the impact point of test

10016 was in front of the center of gravity, it caused a negative rotation about the vertical axis. Figure 16 shows the rotation of both target vehicles each test.

At 200 ms, the target vehicle in test 10010 rotates +30 degrees, while the target vehicle in test 10016 rotates -13 degrees over the same period of time. The maximum rotation at 2 seconds was +130 and -80, respectively.
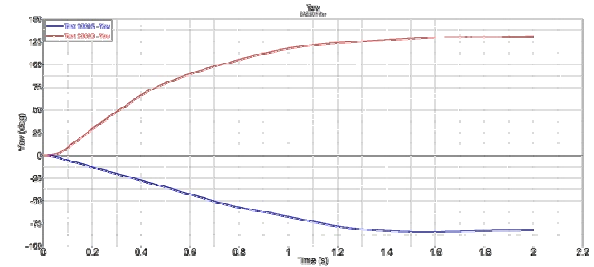
Figure 16: Graph of the rotation of the target vehicles for tests 10010 and 10016. Test 10010 has positive rotation and test 10016 has negative.

Crash pulse analysis

The side-by-side comparison of the crash pulses (Figures 3 and 4) show how different the magnitude and duration of the acceleration can be for different impact locations. For test 10010, the location of the impact was at the B- pillar of the target vehicle. This impact location yields a lower peak acceleration, longer duration crash pulse. In comparison, the impact location of test 10016 was at the A- pillar of the target vehicle. This resulted in a higher peak acceleration, shorter duration crash pulse.

These results show how different areas of the target vehicle have different stiffness. The area of the vehicle around the B- pillar has less stiffness than the area around the A- pillar.

Belt contact analysis

The performance of the seatbelt in far-side impact tests was addressed in this study. In both tests the lap belt maintained contact with the occupant and kept the occupant in the driver seat. However, the shoulder belt lost contact

and the occupant slid out of position. Figure 17 shows the occupant in test 10010 at impact as well as the occupant at 170 ms after impact.

Figure 17: Two frames from test 10010 showing the occupant-seatbelt contact at vehicle impact (above) and after 170 ms. (below)

In both tests, the shoulder of the occupant slides underneath the shoulder belt and the upper body continues to move towards the striking vehicle. For both tests, the occupant loses contact with the shoulder belt between 80 and 90 ms into the event. Test 10016 did not have a video camera on the hood due to its instability in that crash configuration. The video analysis of the Hybrid III head resultant data from Test 10016,shows a steep drop in acceleration around 80 ms. (See Figure 18.) Since the vehicle is accelerating, and accelerating the occupant's head via the contact with the

shoulder belt, the loss in acceleration indicates that the shoulder belt loses contact with the occupant. Since the contact is lost, the force of the belt on the occupant is effectively zero, causing the occupant head acceleration to decrease.
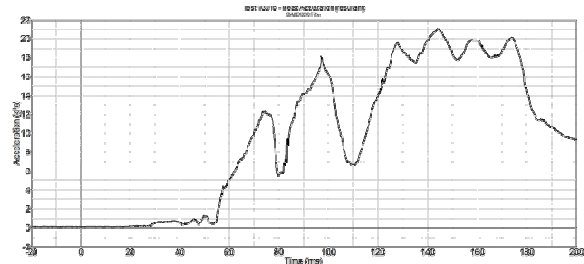
Figure 18: Head resultant acceleration for Hybrid III occupant (Test 10016)

Based on the analysis of video and acceleration data, the rotation of the vehicle at the instant the shoulder belt loses contact with the occupant can be determined. For test 10010, the rotation at 80 ms was +4.4 degrees. For test 10016, the rotation at 80 ms was -3.8 degrees. This difference is very important because it illustrates the direction of a free moving occupant in relation to the motion of the vehicle.

Occupant Motion

Earlier research on computer modeling by Alonso indicated that the existing dummies used in the frontal standards do not replicate the human motion in a far-side impact very well [Alonso, 2007]. However, Alonso found that the human MADYMO human facet model was a good surrogate for a human in far-side tests. For both of the tests, the occupant data was determined using the MADYMO models. The crash environment for the occupant was determined by calculating the angle of the acceleration components and using these as input data. In addition, the direction of the vehicle can be determined with the same lateral and longitudinal components. Finally, the model predicts the angle of the occupant in relation to the vehicle.

The angle of motion of the occupant relative to the vehicle was calculated for each test. For test

10010, the angle of the occupant was 35 degrees (average over 200ms) relative to the longitudinal axis of the vehicle. Visually, this can be seen in Figure 19.

The angle of motion of the occupant relative to the vehicle was also calculated for test 10016. The angle of motion for the occupant in this test was 15 (average over 200ms) degrees relative to the vehicle. This can be seen in Figure 20.
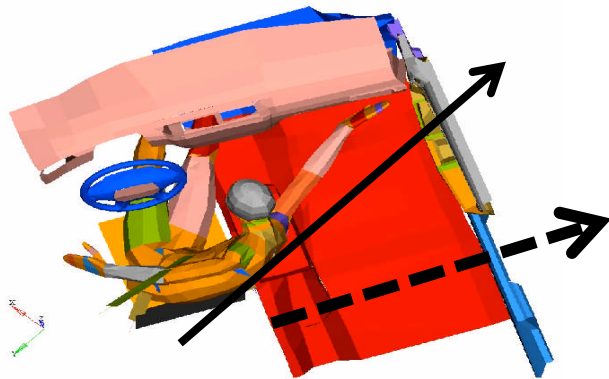
Figure 19: Top view of occupant in MADYMO model (Test 10010). The arrows show the direction of the dummy motion.
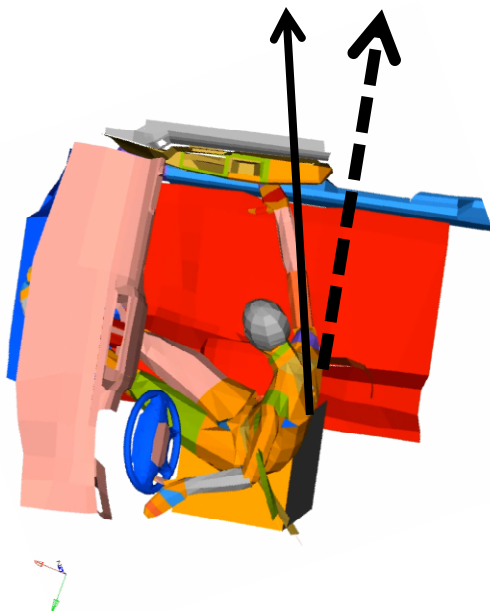
Figure 20: Top view of the occupant in MADYMO model (Test 10016). The arrows show the direction of the human motion

The differences in angles show that the rotation and impact points of the vehicles vary the direction of the occupant motion. In addition, since the shoulder belt was ineffective in both cases, any impact location/angle combination in between these would result in an ineffective shoulder seat belt. Thus, the two tests in this study have different impact points. Any location in between these impact points would result in a loss of seatbelt performance. However, these two impact points are not the upper and lower limits of the area for seatbelt performance loss. Other tests at other locations beyond the A- or B- pillars could also result in an ineffective shoulder belt.

CONCLUSIONS

Further research of far-side impacts is essential to closing the gap in transportation safety. Since there is no government requirement in the United States for occupant safety in far-side seating positions, studies like this must be conducted to show how injuries can occur and how to conduct tests of safety systems to prevent these injuries. From the data and high speed video, we can see that occupants seated in the far side are vulnerable to many types of injuries. Most of these injuries occur because shoulder belts are entirely ineffective in these types of impacts.

Two crash tests were conducted by the National Crash Analysis Center. These tests focused on the occupant seated on the far-side. Acceleration data was recorded for both the vehicle and in one case, the occupant. The data was analyzed, and the kinematics of the occupant was calculated. The use of MADYMO modeling aided in the analysis of the occupant kinematics when data or video view angles were not available.

Analyses of the rotation of the vehicles show how the impact points affect the magnitude of yaw during the collision. For a passenger side impact point behind the center of gravity, the vehicle will rotate positively about the vertical axis, while a passenger side impact point in front of the center of gravity will cause the vehicle to

rotate negatively about the vertical axis. This rotation causes the occupant to move in different directions relative to the vehicle motion.

The MADYMO simulations show that for positive rotation, as seen in test 10010, the occupant will have a larger longitudinal (+x) component of motion. In other words, the occupant will move further forward towards the front of the vehicle. (See Figure 19.) Conversely, the simulations show that for negative vehicle rotation, as in test 10016, the occupant will have more lateral acceleration (+y) and will move towards the far-side door or interior. (See Figure 20). Understanding how the vehicle rotates is important because it can provide a correlation between motion and injury. For example, in a collision like test 10016 where the occupant moves towards the passenger door, the interior of the target vehicle can be displaced towards the occupant. This decreases the distance between the occupant's head and stiff objects in the vehicle that would cause injury. In test 10016, a 62 kph impact, the high speed video shows that the intrusion into the passenger compartment was almost enough to cause the occupant's head to strike the passenger door.

In comparison, a positive rotation as in test 10010, the occupant will move forward towards the center dash or the passenger airbag. This places the occupant in a dangerous position, with their head close to a rapidly deploying airbag. While SRS systems are very beneficial for saving lives in frontal impacts, when occupants are out of place, it can lead to more injury than benefit. High speed video shows the passenger airbag deployment in test 10010 coming very close to the occupant's head while in motion towards the near-side. Rotation analysis like this can lead to further understanding to why specific injuries occur.

In addition to head injuries, the high speed video and MADYMO simulations both indicate a possible upper extremity injury on the near-side. As seen in Figures 19 and 20, the right arm was highly extended towards the near-side. This causes high forces on the shoulders and

possible injury. Gabler [2005] reported that Upper Extremity injuries were second to Head injuries as a source of injury Harm to belted occupants in far-side crashes.

Further research into the occupant motion in far-side impacts can be done. For example, more MADYMO simulations can be completed in conjunction with finite element analysis to examine how vehicle intrusion can affect occupant injury. Also, more impact points and impact angles can be adjusted to find the upper and lower bounds of shoulder belt performance. This kind of research can fine tune the supplemental restraint systems and encourage the adoption of countermeasures..

REFERENCES

Alonso, B., Digges, K., and Morgan, R. (2007) Far-side vehicle simulations with MADYMO. SAE 2007-01-0378, April 2007.

Cuadrado, J. (2008) Comparison of crash pulses and sled responses for far-side impacts. M.S. thesis, Civil & Environmental Engineering Department, The George Washington University, Washington, D. C., 2008.

Cuadrado, J., Smyth, B., Smith, J., and Digges, K., (2010) Validation of sled tests for far-side occupant kinematics using MADYMO. SAE 2010-01-1160, 2010.

Digges, K., Echemendia, C., Fildes, B., and Pintar, F. (2009) A safety rating for far-side crashes. Paper Number 09-0217, Proceedings ESV, June 2009.

Digges, K., Gabler, H., (2006) Opportunities for reducing casualties in far-side crashes. SAE 2006-01-0450, April 2006.

Fildes, B., and Digges, K., (2009), Occupant protection in far-side crashes. Report by George Washington University and Monash University, June 2009.

Fildes B., Gabler H.C., Fitzharris M. & Morris A.P. (2000). Determining side impact priorities

using real-world crash data and harm, Pr IRCOBI, September 2000.

Fildes B., Lane J., Lenard J. & Vulcan, A.P., (1994), Passenger cars and occupant safety: side impact crashes. Report CR134, Australian Transport Safety Bureau (formerly the Federal Office of Road Safety), Canberra, Australia.

Gabler, H., Digges, K., Fildes, B., and Sparks, L. (2005) Side impact injury risk for belted far-side passenger vehicle occupants. SAE 2005-01-0287, April 2005.

Gabler, H., Fitzharris, M., Scully, J., Fildes, B., Digges, K., Sparke, L., (2005) Far-side impact risk for belted occupants in Australia and the United States. Paper 05-0420, ESV Conference, June 2005.

Newland, C., Belcher, T., Bostrom, O., Gabler, H., Cha., J., Wong, H., Tylko, S., and Dal Nevo, R. (2008) Occupant-to-occupant interaction and impact injury risk in side impact crashes. Stapp Car Crash Conference, October 2008.

Pintar, F., Yoganandan , N., Stemper, B., Bostrom , O., Rouhana , S., Digges, K., Fildes, B. (2007) Far-side impact response and dummy biofidelity. Proceedings of the 2007 Stapp Car Crash Conference, October 2007.

Smyth, B and Smith J. (3007) Developing a sled test from crash test data. SAE. 2007-01-0711, 2007.

Society of Automotive Engineers (SAE): Standard J211-1 (1988). Instrumentation for Impact Test, October, 1988.

Selected figures enlarged:
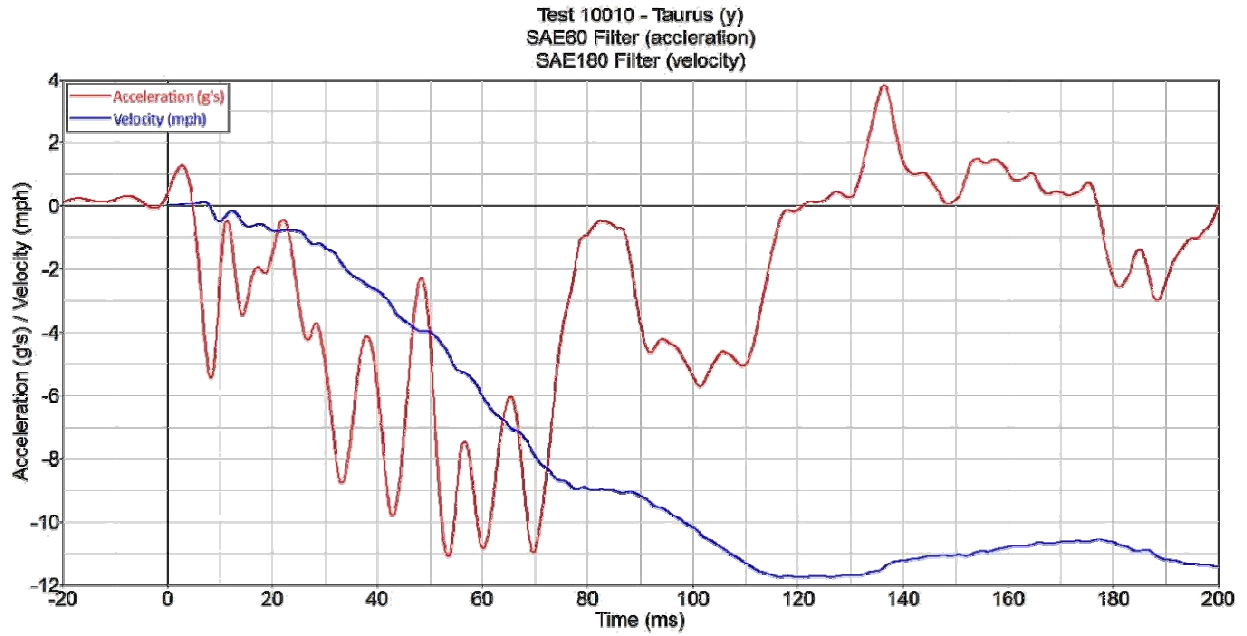
Figure 3
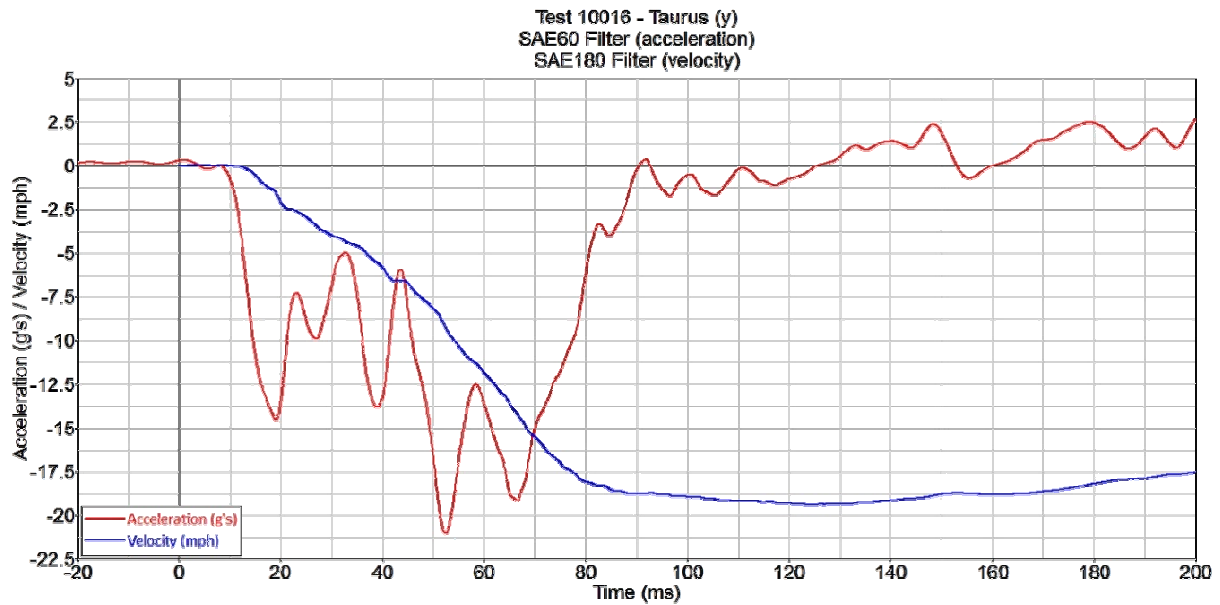
Figure 4
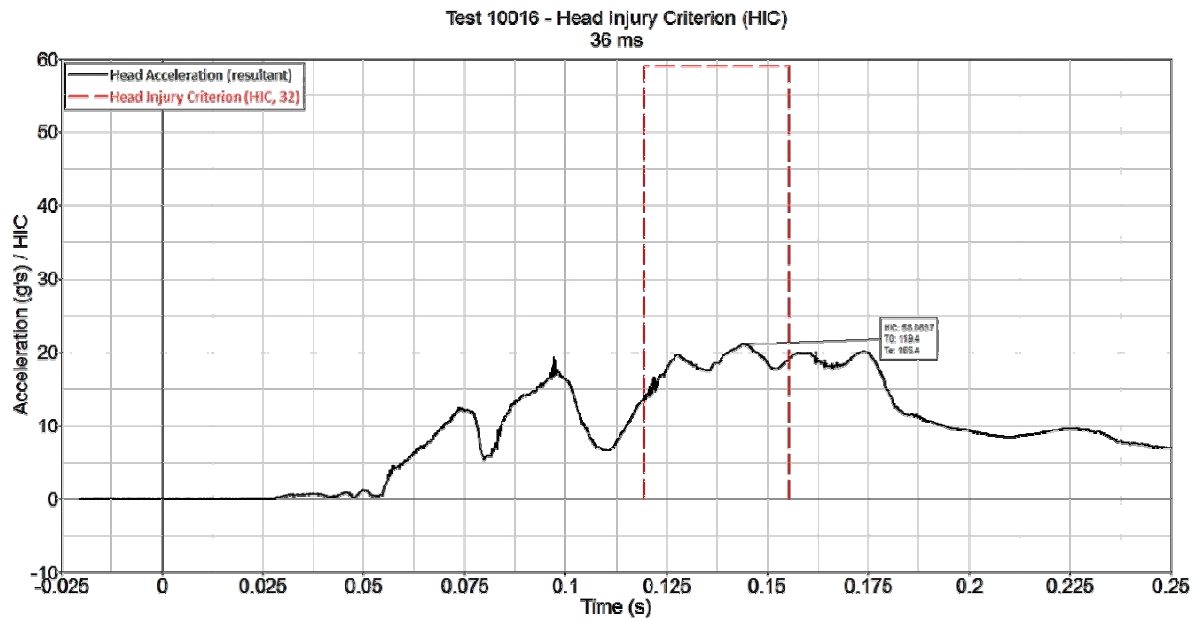
Figure 5
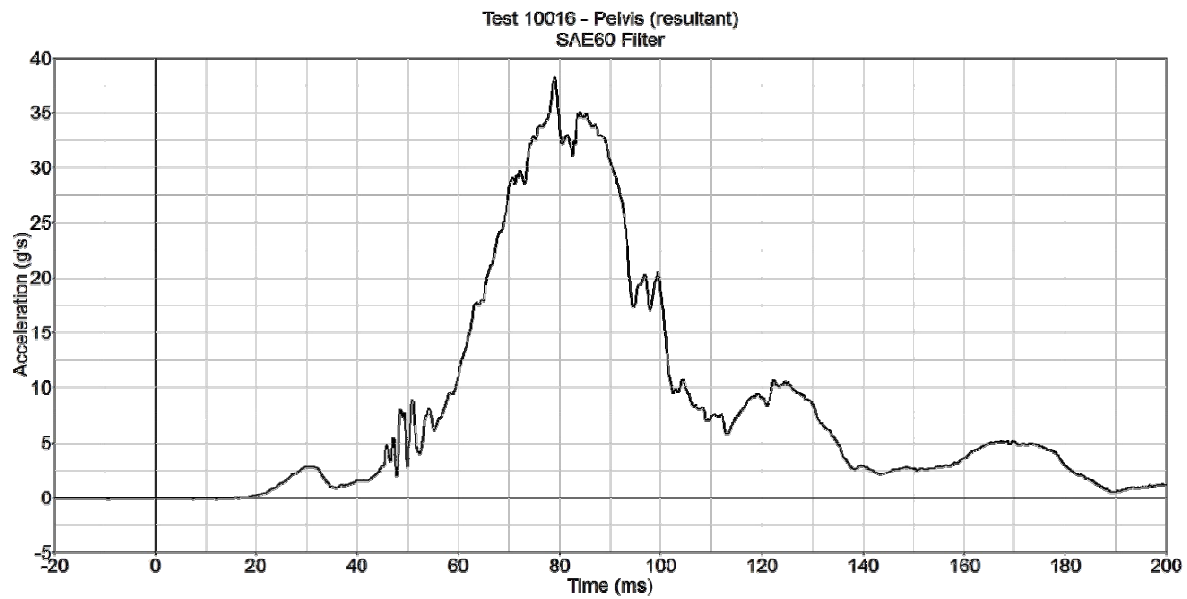
Figure 6

Figure 16

Figure 18